J Nanopart Res (2023) 25:242
https://doi.org/10.1007/s11051-023-05899-9

RESEARCH PAPER

Effect of crystal orientation and temperature on the mechanical properties and fracture mechanism of silicon carbide nanowires

Mengan Cao · Zhaofeng Chen · Le Lu · Shijie Chen · Zhudan Ma · Lixia Yang

Received: 11 August 2023 / Accepted: 15 November 2023 / Published online: 23 November 2023

Abstract Silicon carbide nanowires (SiC NWs) are widely used as reinforcing materials in composite materials based on ceramics, metals, and polymers, and their high-temperature mechanical properties have become a focus of attention. In this paper, the effect of temperature and crystal orientation on the tensile mechanical behavior of SiC NWs was explored through molecular dynamics simulation. It is observed that the fracture mode and mechanical properties of SiC NWs express a significant temperature dependence. Both critical stress and Young's modulus of nanowires with different orientations decrease with increasing temperature and the [111]- and [112]-oriented nanowires exhibit brittle fracture characteristics at low temperatures and become ductile fractures at high temperatures. The transition temperature for ductile–brittle fracture is between 1300-1800 K. The fracture surfaces of SiC NWs with different orientations are all {111} planes at low temperatures. This study provides theoretical support for SiC NWs' laboratory growth and toughening mechanism research.

Keywords Silicon carbide nanowires · Mechanical properties · Fracture mechanisms · Molecular dynamics · Nanocomposites · Modeling and simulation

M. Cao · Z. Chen (✉) · L. Lu · S. Chen · Z. Ma · L. Yang
College of Materials Science and Technology,
Nanjing University of Aeronautics and Astronautics,
Nanjing 211106, People's Republic of China
e-mail: zhaofeng_chen@163.com

Introduction

Due to its quantum size effects, small size effects, surface effects, and macroscopic quantum tunneling effects, one-dimensional silicon carbide (SiC) nanomaterials show better electrical, optical, magnetic, and mechanical properties than macroscopic states [1]. In recent years, it has been found that low-dimensional SiC nanostructures have superior mechanical properties compared to bulk materials. For example, studies have shown that the elasticity and strength of SiC nanowires (NWs) are higher than that of bulk SiC [2], and they are more suitable for bearing tensile and compressive loads. Therefore, SiC NWs are widely used as structural reinforcements of polymers, metals, and ceramic matrix composites [3].

A thorough understanding of the mechanical properties and failure mechanisms of SiC NWs is crucial for their manufacturing and effective execution in various optical and electronic nanodevices, especially in composites where enhancement is achieved through the mechanical response of nanowires. Zhang et al. [4] observed the tensile behavior of single crystal β-SiC nanowires along the crystal direction [111] by in-situ tensile experiment under scanning electron microscopy, and found that the nanowires have a high elongation of 200% due to dislocation generation, slip, propagation, and amorphous. Han et al. [5] found that bending deformation near room temperature can induce the unique mechanical properties of SiC

NWs with large strain plasticity, which has never been observed in bulk ceramic materials. Cheng et al. [6] studied the influence of different defect forms in SiC NWs on their mechanical properties and concluded that the size effect of fracture strength is determined by the size dependent defect density, rather than the surface effect of single crystal nanowires. Yang et al. [7] found that adding SiC NWs into SiC matrix composites can double the fracture toughness and bending strength of the composites, which reflects the excellent mechanical properties of SiC NWs.

Molecular dynamics (MD) simulation, as a powerful tool for studying the mechanical behavior and fracture mechanism of nanomaterials under different load modes, can understand the dynamic process of the origin and evolution of stress-induced damage in nanomaterials at the atomic scale, and has been widely used in the study of the mechanical behavior of various nanomaterials [8–11]. For example, Makeev et al. [12] used Tersoff empirical potential and classical MD simulation to study the mechanical properties of < 111 >—oriented SiC NWs under tensile, compressive, torsional, and bending forces. Wang et al. [13] investigated the tensile behavior of [111]-oriented SiC NWs with different microstructures using MD simulation, and the results showed that the widespread dispersion of mechanical properties observed in the experiment may be attributed to their different microstructures. However, current researches on the mechanical properties of SiC NWs mostly focus on the [111] crystal orientation. Different crystal orientation nanowires have different atomic arrangements, and the atomic arrangement at the micro level of the material determines the macroscopic mechanical properties.

Based on the nanowires successfully prepared in the experiment, three nanowire models with different crystal orientations were constructed in this paper: [001] [14], [111] [14–16], and [112] [17]. The effects of temperature and crystal orientation on the mechanical properties of SiC NWs were studied using molecular dynamics (MD) simulation methods, and the failure mechanism of nanowires under different conditions was elucidated. By exploring the relevant mechanical behavior and fracture mechanism of nanowires with different crystal orientations, theoretical guidance can be provided for SiC NWs' laboratory growth and toughening mechanism research.

Simulation procedures

In MD simulation, the selection of interatomic potential is of vital importance. In the simulation of the SiC covalent bond system, the most widely used potential functions are Stillinger Weber (SW) and Tersoff potential function, both of which are three body potential functions. Tersoff potential function takes into account the influence of covalent bond, bond angle, and atomic local microenvironment on the bond level, which can accurately describe the formation and fracture of covalent bonds and the dynamic process of covalent bond change between atoms, and has been widely used to study the fracture behavior [18, 19], thermal properties [20, 21], amorphous transition [22] and radiation-induced defects [23] of SiC. Therefore, the Tersoff [24] interaction potential function was selected in this study to describe the interatomic interaction, which can be represented as:

$$E = \sum_i E_i = \frac{1}{2} \sum_{i \neq j} V_{ij} \tag{1}$$

$$V_{ij} = f_c(r_{ij}) \left[f_R(r_{ij}) + b_{ij} f_A(r_{ij}) \right] \tag{2}$$

where E denotes the total energy of the system, V_{ij} represents the bonding energy between atom i and atom j, f_A and f_R are the attractive and repulsive terms of the potential, respectively, f_c is the smooth truncation function and b_{ij} is the attractive potential function.

In this study, all simulations were conducted using the Large-scale Atomic/Molecular Massively Parallel Simulator (LAMMPS) [25]. The 3C-SiC nanowire models with [001], [111], and [112] orientations were established. For simplicity, set the cross-sectional shape of the nanowires to circular which is similar to the actual synthesized SiC NWs, and the radius of all nanowires was set at 15 Å and the length at 100 Å, ensuring that the aspect ratio greater than 3:1. Similar aspect ratios have been widely used in previous studies [26–28], and the established models are shown in Fig. 1.

Periodic boundary conditions were applied along the stretching direction (Z axis), and free boundary conditions were set in the other directions. In order to eliminate the unreasonable structure of the initial model and keep the system in equilibrium, the model was thermally equilibrated at 300 K for 50 picoseconds (ps) by

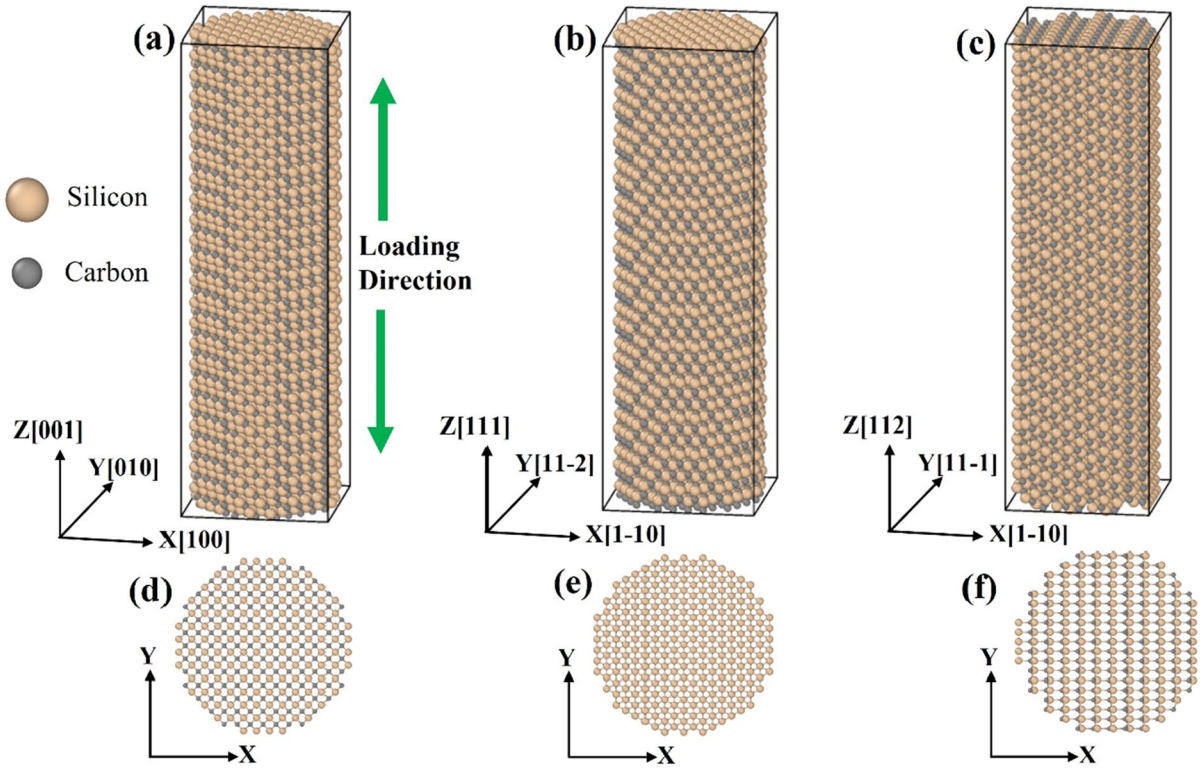

Fig. 1 Atomic model of SiC nanowires with axial orientations of (**a**) [001], (**b**) [111], and (**c**) [112]. The top view of different orientations is shown in (**d**), (**e**), and (**f**), respectively. (The loading direction is also shown in the figure, here, silicon atoms are colored in brown and carbon atoms are colored in gray)

means of the Nose–Hoover thermostat [29] under the NVT ensemble with a timestep of 1 femtosecond (fs). After relaxation, a uniform load was applied along the Z-axis at a strain rate of 5×10^{9} s^{-1} per 1000 steps until the nanowires were pulled off. This strain rate was chosen because studies [30, 31] show that the deformation behavior of the nanowires is not affected by the strain rate when the strain rate is less than 10^{10} s^{-1}.

The average stress P_{zz} along the axis of the nanowires was calculated in the form of virial formula [32]:

$$P_{zz} = \frac{\sum_i^N m_i v_{iz}^2}{V} + \frac{\sum_i^N r_{iz} f_{iz}}{V} \tag{3}$$

where V represents the volume of the system, m_i and viz denote the mass and velocity of the ith atom along the axial direction, r_{iz} and f_{iz} are the corresponding position and force of the ith atom along the axial direction. The strain is calculated according to the definition of engineering strain, i.e.$\varepsilon = \left(l - l_0\right)/l_0$, where l is the length of the stretched nanowire and l_0 is the initial length.

Results and discussions

Effect of temperature on mechanical properties and fracture mechanism of SiC NWs with different orientations

In order to investigate the influence of temperature on the fracture mode of SiC NWs, the deformation behavior of different oriented nanowires under the same loading conditions was analyzed at 300 K, 800 K, 1300 K, and 1800 K. Figure 2 shows the stress–strain curves of SiC NWs with different orientations at different temperatures. It can be seen from Fig. 2(a) that the stress–strain curves of the [001] SiC NWs exhibit the same change trend at different temperatures. At the beginning of loading, SiC NWs show linear elastic deformation, and the stress–strain curve increases linearly up to a strain value of 6%, upon further stretching, the nanowires begin to show non-linear elasticity, and the slope of the curve decreases gradually. However, the nanowires still

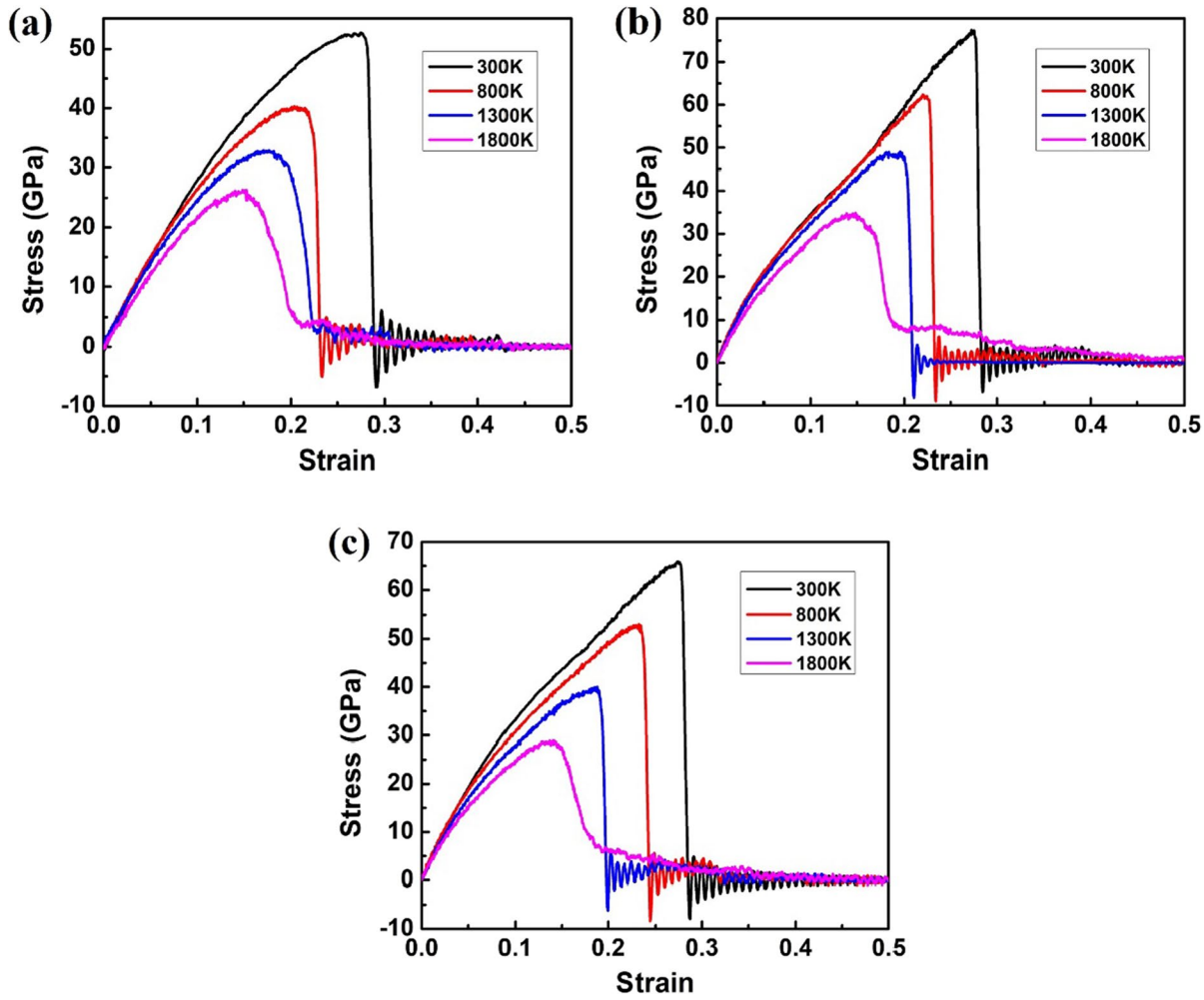

Fig. 2 The tensile stress–strain curves of the (**a**) [001], (**b**) [111], (**c**) [112] SiC NWs at different temperatures

have the ability to resist deformation, and the stress still increases with the increase of the strain, which is similar to the strengthening stage of metal materials. The stress drops suddenly after reaching critical strain and the nanowires fracture. It is preliminarily believed that [001] SiC NWs exhibit ductile fracture characteristics at different temperatures. Using the least square method to linearly fit the 0 ~ 5% strain region at 300 K, and the curve slope is 314, that is, the Young's modulus of the nanowire is 314 GPa. This result is in good agreement with the result of 338 GPa obtained by W.Li [33] et al. based on the pseudopotential plane wave method and local density functional theory, and the result of 362 GPa obtained by Lambrecht et al. [34] based on full potential linear Muffin-Tin orbits combined with local density functional theory.

For [111] crystal direction, as illustrated in Fig. 2(b), when the temperature is below 1300 K, the stress of nanowires increases linearly with the increase of strain until it reaches the critical stress. With the further increase of strain, the stress suddenly drops to zero, showing a typical brittle fracture characteristic. However, after the stress increases to the critical stress with strain at 1800 K, and with the further increase of the strain, the stress slowly decreases and undergoes a large strain process before decreasing to 0, exhibiting ductile type fracture characteristics. It can be observed that the fracture mode of [111]-oriented nanowires is related to the external

temperature, showing the fracture characteristics of low-temperature brittle fracture and high-temperature ductile fracture, and the brittle-ductile transition temperature is between 1300-1800 K. Similarly, fitting the linear stage of the stress–strain curve at 300 K leads to the Young's modulus of 406.55 GPa for the nanowire. Petrovic et al. [35] measured the Young's modulus of [111]-oriented SiC nanowires using a specially developed micro tensile tester, which ranged from 361 to 890 GPa, showing strong dispersion, indicating that our simulation results are reasonable. It can be seen from Fig. 2(c) that the [112]-oriented nanowires exhibit the same fracture characteristics as the [111]-oriented nanowires, namely brittle type fracture at low temperatures and ductile type fracture at high temperatures.

The fracture mode was analyzed by combining the atomic configuration diagrams before and after the fracture of nanowires during stretching to further illustrate the effect of temperature on the fracture mode of SiC NWs. Figure 3 shows the fracture mode of [001]-oriented nanowires at temperatures of 300 K (Fig. 3(a)) and 1800 K (Fig. 3(b)). It can be observed that the nanowires show a necking phenomenon before breaking at different temperatures, and monoatomic chains appear after breaking, which is similar to the results of CdSe NWs [32] and shows the characteristics of ductile fracture.

Figure 4 shows the atomic configuration diagrams of [111] and [112]-oriented nanowires at different strain stages at 300 K and 1800 K, respectively. It can be seen that the two nanowires with different orientations exhibit the same fracture characteristics. As illustrated in Fig. 4(a) and (c), when the strain reaches the critical strain at 300 K, the Si–C bond breaks suddenly without necking, and the fracture section is relatively flat, perpendicular to the loading direction, which indicates that the nanowire is brittle fracture. It can be seen from Fig. 4(b) and (d) that a significant necking phenomenon occurs during the stretching process of the nanowire at 1800 K. For [111]-oriented nanowire, the surface atomic bonds fracture at a strain of 25%. As the strain further increased, the nanowire undergoes significant plastic deformation, and the atomic bonds do not fracture on a large scale until the strain reaches 45%. At this time, the nanowire failed and exhibits obvious ductile fracture characteristics. The atomic configuration diagram during the stretching process of SiC NWs further proves that [111] and [112]-oriented nanowires fracture in a brittle type at low temperatures and in a ductile type at high temperatures.

The Young's modulus and critical stress of nanowires with different orientations at different temperatures were calculated to explore how the temperature affects the mechanical properties of SiC NWs, as shown in Table 1. It can be seen that the mechanical properties of nanowires exhibit significant temperature dependence. For example, for [001]-oriented nanowires, as the temperature increases from 300 to 1800 K, Young's modulus decreases from 314 GPa to 249.24 GPa, fracture

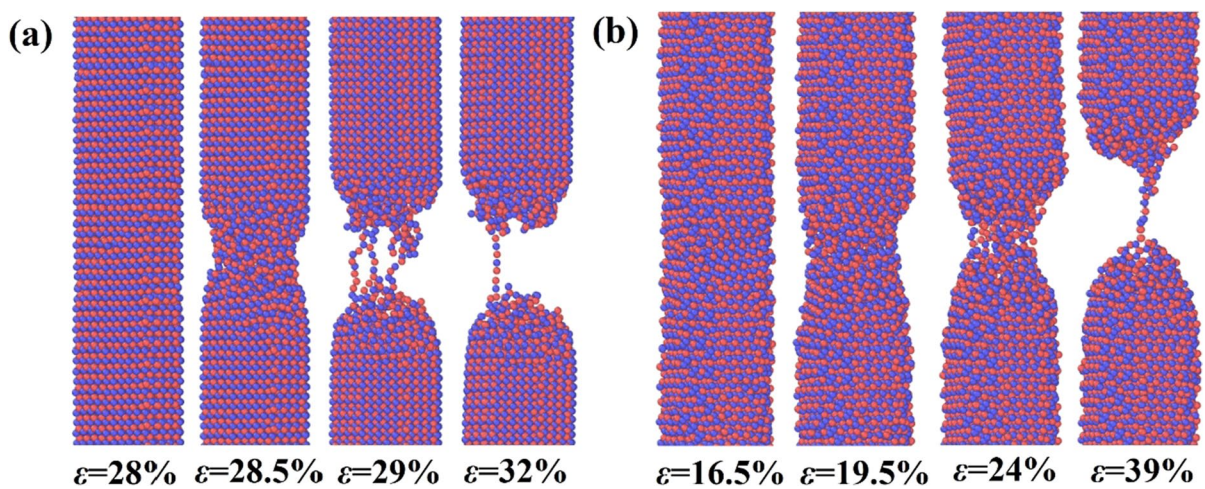

Fig. 3 Atomic configuration diagram of [001] SiC NWs for various strain levels at (**a**) 300 K and (**b**) 1800 K

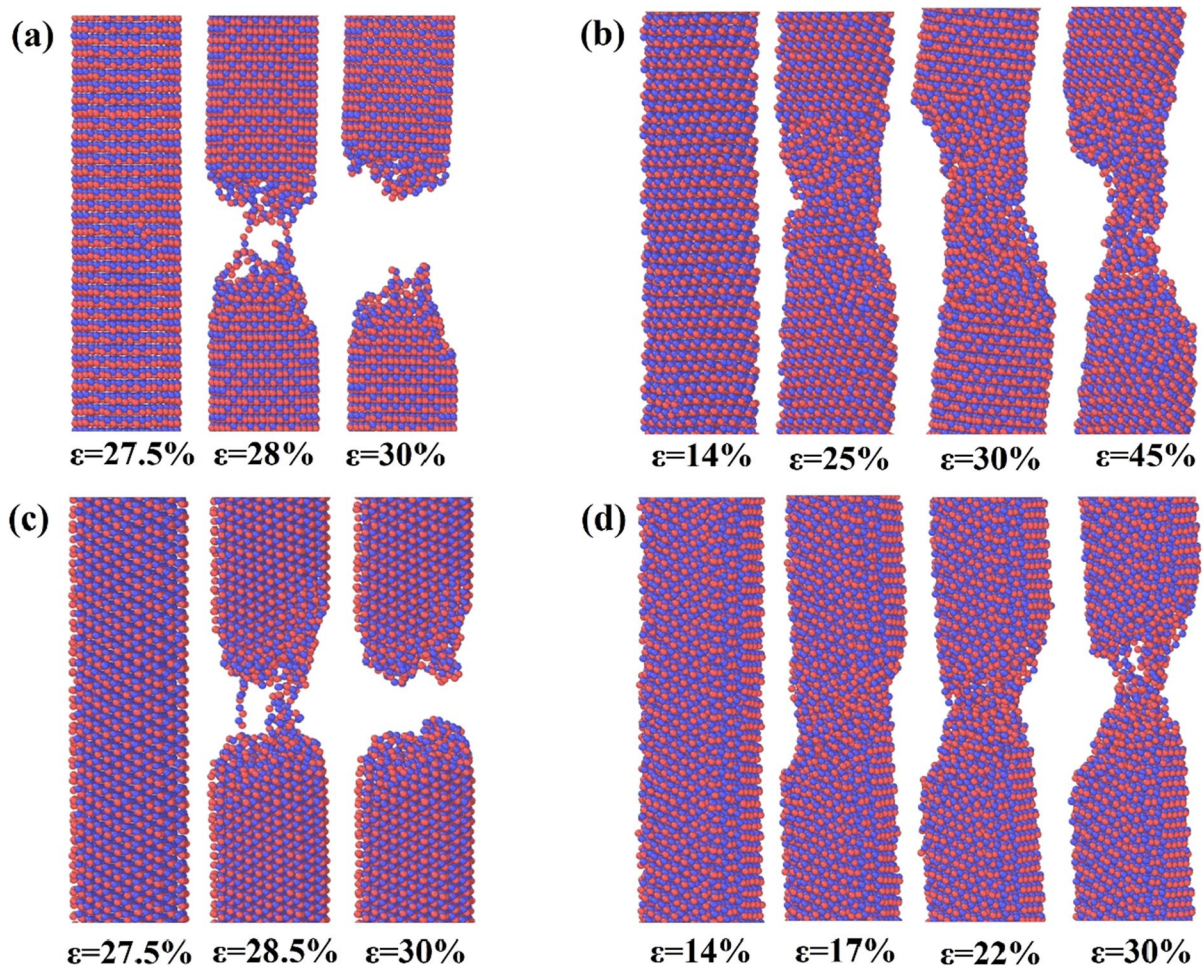

Fig. 4 Atomic configuration diagram of [111] SiC NWs for various strain levels at (**a**) 300 K and (**b**) 1800 K, and [112] SiC NWs for various strain levels at (**c**) 300 K and (**d**) 1800 K

strength decreases from 52.75 GPa to 26.3 GPa, and both the Young's modulus and critical stress decrease with increasing temperature. This phenomenon can be explained as the energy of atoms increases and the vibration amplitude intensifies as the temperature increases, which makes it easy for atoms to detach from the normal lattice position and causes the atomic bonds to fully elongate, increasing the possibility of the atomic bonds reaching the critical bond length. Therefore, as long as a small tensile force is applied, the bond fracture will occur, indicating that the thermal activation process contributes greatly to the complete elongation of SiC NWs.

Table 1 The young's modulus and critical stress of SiC NWs with [001], [111],[112] orientation at different temperatures

Orientation	Young's modulus (GPa)				Critical stress (GPa)			
	300 K	800 K	1300 K	1800 K	300 K	800 K	1300 K	1800 K
[001]	314	298.46	273.42	249.24	52.72	40.3	32.88	26.3
[111]	406.55	402.5	392.97	344.43	77.46	62.33	49.30	34.85
[112]	380.43	362.61	334.79	294.66	65.88	53.05	40.01	28.86

The potential energy distribution of per atom for [001]-oriented nanowires at different temperatures was studied to obtain more information about the effect of temperature on the mechanical properties of SiC NWs. It can be seen from Fig. 5 that no matter what the temperature is, the surface atoms always have high energy. This is because the low coordination number of the surface atoms makes them easy to combine with other atoms and have high activity. When the nanowire is loaded, the surface atoms are easy to become the nucleation zone of crack defects, and the cracks evolve from the surface to the interior, resulting in the fracture failure of the nanowire. However, the number of atoms with high potential energy in the center of the nanowire gradually increases with the increase of temperature, making the nanowire unstable and increasing the possibility of internal crack defects, making fracture more likely to occur and leading to a decrease in the mechanical properties.

Effect of crystal orientations on the mechanical properties and fracture mechanism of SiC NWs

The stress–strain curves of SiC NWs with [001], [111], and [112] orientations at 300 K are shown in Fig. 6(a). It can be observed that the fracture strain of nanowires with different orientations is approximately the same, all around 27%, however, by measuring the area below the stress–strain curve, it is found that [111]-oriented SiC NWs have the maximum fracture toughness, which means that they need to consume more energy before fracture and have higher resistance to fracture, while the minimum fracture toughness is obtained for [001]-oriented SiC NWs. The changes in critical stress and Young's modulus of different oriented nanowires with temperature are shown in Fig. 6(b) and (c) respectively. It is observed that regardless of temperature, [111]-oriented nanowires always exhibit the maximum Young's modulus and critical stress, followed by [112] and [001]-oriented nanowires, indicating that the mechanical properties of nanowires have strong orientation dependence. Similar research results have also been reported in the study of Si [36] and CdSe [37] nanowires.

The reason why SiC NWs with different crystal orientations show different mechanical properties is mainly that nanowires with different orientations have different outer surfaces, corresponding to different surface energies [38, 39]. Besides, the bonding state of surface atoms is different from that of internal atoms, and the mismatch of bonding states of surface atoms results in the softening of intrinsic stress on elastic modulus. It has been reported [39–41] that among the three orientations, [111] SiC NWs have the largest surface atomic distance, thus the minimum surface atomic density, which allows it to have the lowest surface energy and the most stable atomic structure. In addition, the minimum surface atomic density leads to the lowest

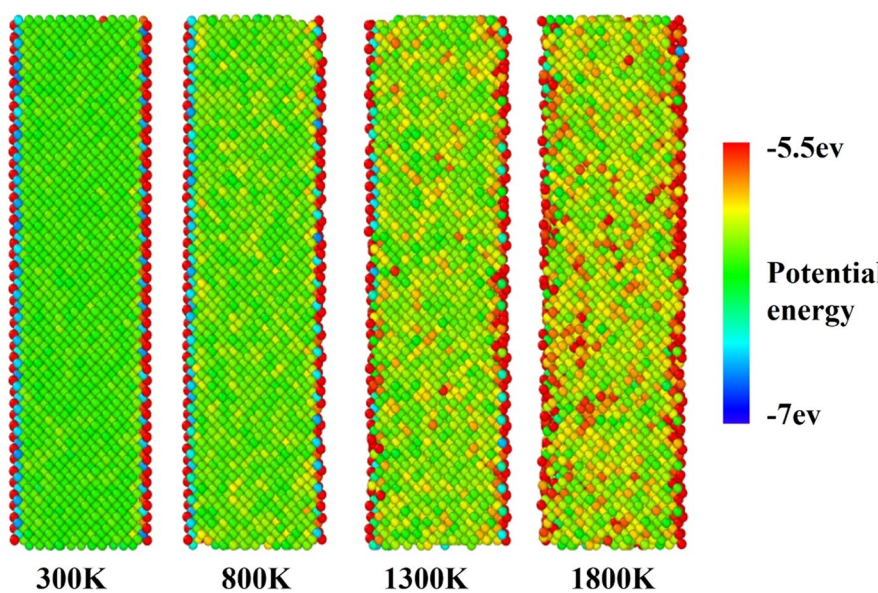

Fig. 5 Potential energy distribution of per atom for [001] SiC NWs at different temperatures

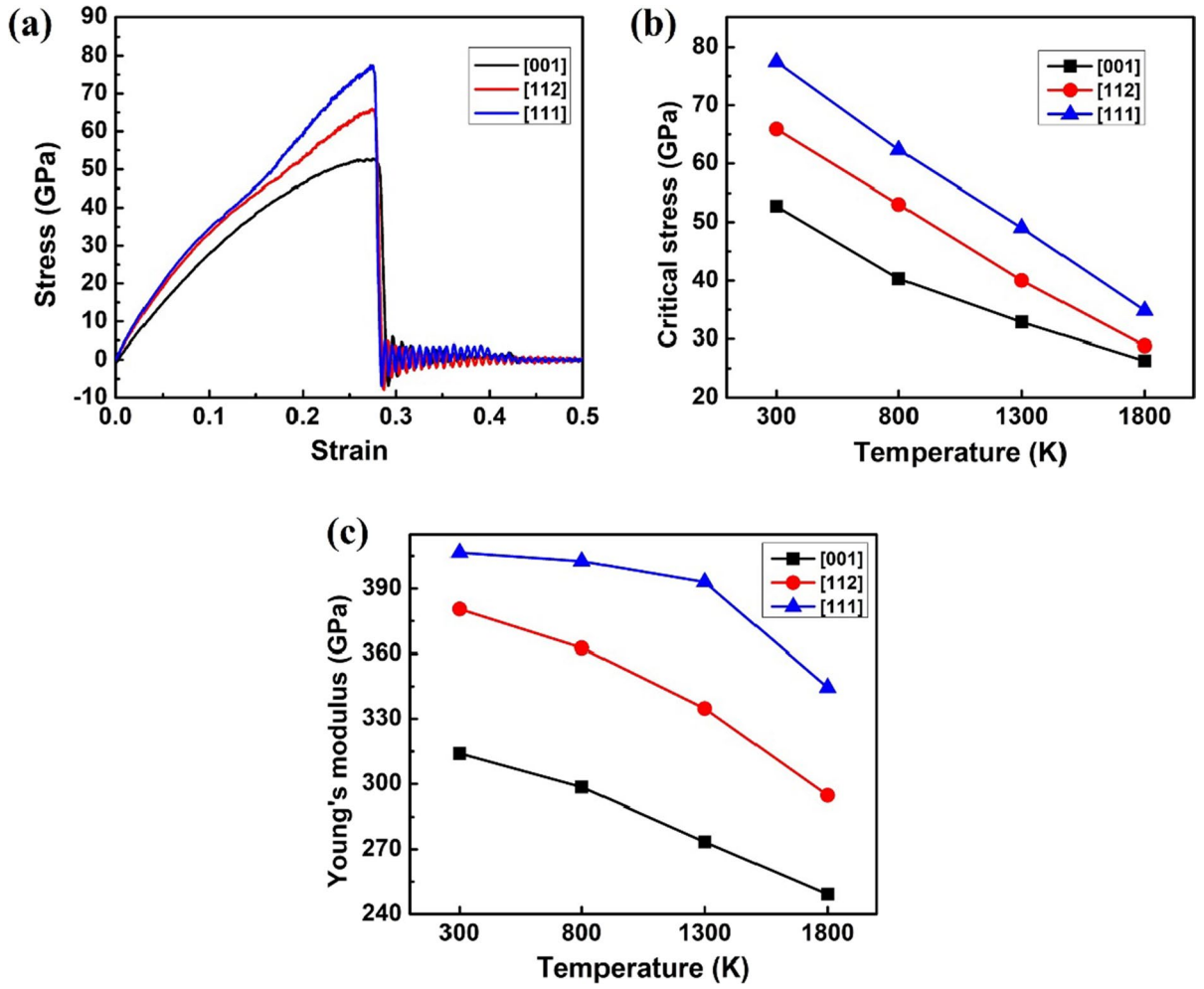

Fig. 6 (**a**) Stress–strain curves of SiC NWs for different orientations at 300 K. Variations of Critical stress (**b**) and Young's modules (**c**) with temperature for nanowires with different orientations

softening effect of the intrinsic stress and the largest elastic modulus, followed by [112] and [001] orientations. What's more, the lowest surface energy of the [111] SiC NWs endows it with the highest fracture resistance and therefore has the highest tensile strength.

Then, the failure mechanism of nanowires with different orientations at 300 K was investigated. In order to understand the nucleation process of cracks more clearly, the DIA (identify diamond structure) atomic recognition method was adopted to identify and color the crystal structure, as shown in Fig. 7. The generation of Other type atoms indicates that the stress concentration caused by local defects leads to the atoms detaching from their normal lattice positions and having unknown coordination structures, resulting in the fracture of atomic bonds and the formation of cracks.

For the [001]-oriented SiC NWs, it can be seen from Fig. 7(a-I) that the cracks form on the surface at the strain of 27%. With the further increases of the strain, cracks begin to expand and branch, and large-scale failure occurs at 28.8% strain, at which point the nanowires fail. Combining Fig. 7(a-II) and (a-III) can provide a clearer understanding of the crack propagation direction. Observing from the x–z and y–z planes, it was found that the fracture plane always has a 45° angle with the nanowire axis, indicating that the fracture occurred along the {111} planes [42–44].

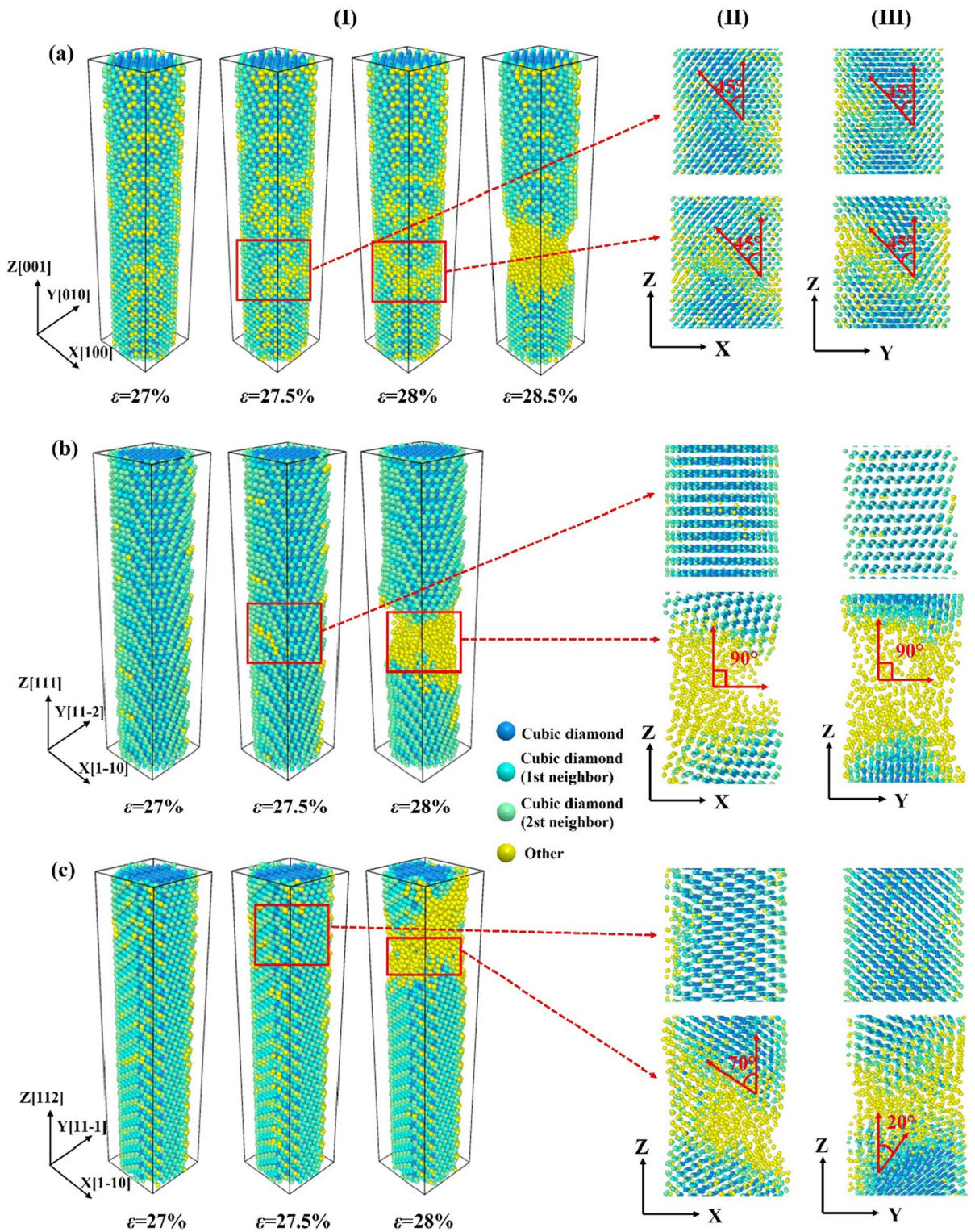

Fig. 7 Failure mechanism of (**a**) [001], (**b**) [111], and (**c**) [112] SiC NWs at 300 K. The figures in columns (II) and (III) represent the crack nucleation direction of the corresponding strain stages shown in column (I) from different perspectives, atoms' size is reduced for better visualization. Atoms are colored according to their diamond structure

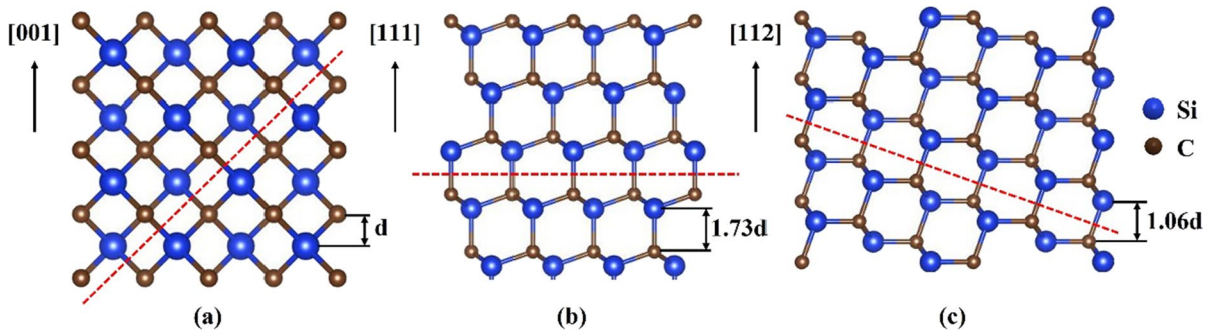

Fig. 8 Representations of atomic arrangements of SiC NWs with different crystal orientations. Dotted lines represent the crack nucleation direction of nanowires under load

As can be seen from Fig. 7(b-I) and (c-I), the fracture characteristics of the [111] and [112]-oriented SiC NWs are different from that of the [001]-oriented. There is no crack propagation phenomenon before fracture, but failure occurs immediately after reaching the critical strain, further verifying that the [001]-oriented nanowires fracture in a brittle type. By observing the nucleation direction of cracks in Fig. 7(b-II) and (b-III), it is found that the fracture plane of the [111]-oriented nanowire is always perpendicular to the axial direction, indicating that cleavage fracture occurred along the {111} planes. By observing Fig. 7(c-II) and (c-III), it is found that the fracture plane makes a 70° angle with the axial direction in the x–z plane, while makes a 20° angle with the axial direction in the y–z plane. Through calculation, it was found that the angle between the [112] and [111] crystal orientations is 20°, indicating that the angle between the [112] crystal orientations and the {111} planes is 70°, which is consistent with the observed angle, indicating that the [112]-oriented nanowires also fracture along the {111} planes.

Studies have shown that the bond breaking in the cleavage plane mainly depends on the surface polarity, atomic bond length, and coordination number [45]. To explain the fracture mechanism of nanowires, the atomic arrangement patterns corresponding to different crystal orientations of SiC NWs (Fig. 8) were provided. It can be seen that the maximum plane spacing corresponding to the [001], [111], and [112]-oriented nanowires are at an angle of 45°, 90°, and 70° to their axis, respectively. The large spacing between planes leads to a decrease in interatomic forces, resulting in a decrease in the energy required for crack nucleation. Therefore, the crack propagates in different directions, forming fracture planes at different angles, consistent with the results observed in Fig. 7

Conclusions

The effects of temperature and crystal orientation on the tensile mechanical behavior of SiC NWs have been studied through molecular dynamics simulation in this investigation. The results indicate that the fracture mode and mechanical properties of SiC NWs exhibit significant temperature dependence. With the increase of temperature, the critical stress and Young's modulus of nanowires with different crystal orientations will decrease due to the surface effect and the soft effect induced by high temperature. For [111] and [112]-oriented nanowires, they exhibit brittle fracture characteristics at low temperatures and become ductile fracture at high temperatures. The transition temperature for ductile–brittle fracture is between 1300-1800 K. In addition, it is found that there are great differences in mechanical properties of nanowires with different crystalline orientations. Regardless of the temperature, [111]-oriented nanowires always show the highest critical stress, Young's modulus, and fracture toughness, followed by [112] and [001] crystal orientation. However, it is observed that the nanowires with different orientations break along the {111} plane at low temperatures. Combined with the atomic arrangement, it is found that the {111} plane presents the largest plane spacing and the minimum energy required for crack nucleation. This

study provides a detailed introduction to temperature and crystal orientation-dependent mechanical properties and fracture mechanisms of SiC NWs, hoping to provide theoretical guidance for the structural design of nanowires in experiments.

Acknowledgements This research work was supported by the National Natural Science Foundation of China (92160202), the National Key Research and Development Plan of China (2021YFB3703100), and the Ningbo key technology Research and Development(2023T007).

Author contribution Mengan Cao: Conceptualization, Data curation, Formal analysis, Investigation, Methodology, Resources, Validation, Visualization, Writing – original draft. **Zhaofeng Chen:** Funding acquisition, Project administration, Supervision, Validation, Writing – review & editing. **Le Lu:** Validation, Writing – review & editing. **Shijie Chen:** Writing – review & editing. **Zhudan Ma:** Writing – review & editing. **Lixai Yang:** Funding acquisition, Writing – review & editing.

Funding This research work was supported by the National Natural Science Foundation of China (92160202).

Data availability Data will be made available on request.

Declarations

Competing interest The authors declare that they have no known competing financial interests or personal relationships that could have appeared to influence the work reported in this paper.

References

1. Chen S, Li W, Li X, Yang W (2019) One-dimensional SiC nanostructures: Designed growth, properties, and applications. Prog Mater Sci 104:138–214
2. Wong EW, Sheehan PE, Lieber CM (1997) Nanobeam mechanics: Elasticity, strength, and toughness of nanorods and nanotubes. Science 277:1971–1975
3. Guo C, Cheng LF, Ye F (2019) Research and application development of SiC nanowires. Mater China 38:831–842+886
4. Zhang Y, Han X, Zheng K, Zhang Z, Zhang X, Fu J, Ji Y, Hao Y, Guo X, Wang ZL (2007) Direct observation of super-plasticity of Beta-SiC nanowires at low temperature. Adv Func Mater 17:3435–3440
5. Han XD, Zhang YF, Zheng K, Zhang XN, Zhang Z, Hao YJ, Guo XY, Yuan J, Wang ZL (2007) Low-temperature in situ large strain plasticity of ceramic SiC nanowires and its atomic-scale mechanism. Nano Lett 7:452–457
6. Cheng G, Chang T-H, Qin Q, Huang H, Zhu Y (2014) Mechanical properties of silicon carbide nanowires: Effect of size-dependent defect density. Nano Lett 14:754–758
7. Yang W, Araki H, Tang C, Thaveethavorn S, Kohyama A, Suzuki H, Noda T (2005) Single-crystal SiC nanowires with a thin carbon coating for stronger and tougher ceramic composites. Adv Mater 17:1519–1523
8. Mandal T (2012) Strain induced phase transition in CdSe nanowires: Effect of size and temperature. Appl Phys Lett 101(2):021906
9. Wang Z, Zu X, Gao F, Weber WJ (2008) Atomistic simulations of the mechanical properties of silicon carbide nanowires. Phys Rev B 77:224113
10. Konuk M, Durukanoğlu S (2012) Strain-induced structural transformation of a silver nanowire. Nanotechnology 23:245707
11. Kulkarni AJ, Zhou M, Ke FJ (2005) Orientation and size dependence of the elastic properties of zinc oxide nanobelts. Nanotechnology 16:2749
12. Makeev MA, Srivastava D, Menon M (2006) Silicon carbide nanowires under external loads: An atomistic simulation study. Phys Rev B 74:16
13. Wang J, Lu C, Wang Q, Xiao P, Ke F, Bai Y, Shen Y, Liao X, Gao H (2012) Influence of microstructures on mechanical behaviours of SiC nanowires: a molecular dynamics study. Nanotechnology 23:025703
14. Peng HY, Zhou XT, Lai HL, Wang N, Lee ST (2000) Microstructure observations of silicon carbide nanorods. J Mater Res 15:2020–2026
15. Attolini G, Rossi F, Bosi M, Watts BE, Salviati G (2011) The effect of substrate type on SiC nanowire orientation. J Nanosci Nanotechnol 11:4109–4113
16. Krishnan B, Thirumalai RVKG, Koshka Y, Sundaresan S, Levin I, Davydov AV, Merrett JN (2011) Substrate-dependent orientation and polytype control in SiC nanowires grown on 4H-SiC substrates. Cryst Growth Des 11:538–541
17. Sundaresan SG, Davydov AV, Vaudin MD, Levin I, Maslar JE, Tian Y-L, Rao MV (2007) Growth of silicon carbide nanowires by a microwave heating-assisted physical vapor transport process using group VIII metal catalysts. Chem Mater 19:5531–5537
18. Tang M, Yip S (1994) Lattice instability in β-SiC and simulation of brittle fracture. J Appl Phys 76:2719–2725
19. Kikuchi H, Kalia RK, Nakano A, Vashishta P, Branicio PS, Shimojo F (2005) Brittle dynamic fracture of crystalline cubic silicon carbide (3C-SiC) via molecular dynamics simulation. J Appl Phys 98:103524
20. Tang M, Yip S (1995) Atomistic simulation of thermomechanical properties of β-SiC. Phys Rev B 52:15150
21. Porter LJ, Li J, Yip S (1997) Atomistic modeling of finite-temperature properties of β-SiC. I. Lattice vibrations, heat capacity, and thermal expansion. J Nucl Mater 246:53–59
22. Mizushima K, Tang M, Yip S (1998) Toward multiscale modelling: the role of atomistic simulations in the analysis of Si and SiC under hydrostatic compression. J Alloy Compd 279:70–74
23. Gao F, Weber WJ, Posselt M, Belko V (2004) Atomistic study of intrinsic defect migration in 3C-SiC. Phys Rev B 69:245205
24. Tersoff J (1989) Modeling solid-state chemistry: Interatomic potentials for multicomponent systems. Phys Rev B 39:5566
25. Plimpton S (1995) Fast parallel algorithms for short-range molecular dynamics. J Comput Phys 117:1–19

26. Yang Z, Lu Z, Zhao Y-P (2009) Shape effects on the yield stress and deformation of silicon nanowires: A molecular dynamics simulation. J Appl Phys 106:023537
27. Guénolé J, Brochard S, Godet J (2011) Unexpected slip mechanism induced by the reduced dimensions in silicon nanostructures: Atomistic study. Acta Mater 59:7464–7472
28. Guénolé J, Godet J, Brochard S (2011) Deformation of silicon nanowires studied by molecular dynamics simulations. Modell Simul Mater Sci Eng 19:074003
29 Allen MP, Tildesley DJ (2017) Computer simulation of liquids. Oxford University Press
30. Koh S, Lee H, Lu C, Cheng Q (2005) Molecular dynamics simulation of a solid platinum nanowire under uniaxial tensile strain: Temperature and strain-rate effects. Phys Rev B 72:085414
31. Liu Q, Shen S (2012) On the large-strain plasticity of silicon nanowires: effects of axial orientation and surface. Int J Plast 38:146–158
32. Fu B, Chen N, Xie Y, Ye X, Gu X (2013) Size and temperature dependence of the tensile mechanical properties of zinc blende CdSe nanowires. Phys Lett A 377:2681–2686
33. Li W, Wang T (1999) Elasticity, stability, and ideal strength of β-SiC in plane-wave-based ab initio calculations. Phys Rev B 59:3993–4001
34. Lambrecht WRL, Segall B, Methfessel M, van Schilfgaarde M (1991) Calculated elastic constants and deformation potentials of cubic SiC. Phys Rev B 44:3685–3694
35. Petrovic JJ, Milewski JV, Rohr DL, Gac FD (1985) Tensile mechanical properties of SiC whiskers. J Mater Sci 20:1167–1177
36. Kang K, Cai W (2010) Size and temperature effects on the fracture mechanisms of silicon nanowires: molecular dynamics simulations. Int J Plast 26:1387–1401
37. Munshi MAM, Majumder S, Motalab M, Saha S (2019) Insights into the mechanical properties and fracture mechanism of cadmium telluride nanowire. Mater Res Express 6:105083
38. Yang Z, Lu Z, Zhao Y-P (2009) Atomistic simulation on size-dependent yield strength and defects evolution of metal nanowires. Comput Mater Sci 46:142–150
39. Lu H, Zhang J, Fan J (2011) Molecular dynamics study of the tensile mechanical behavior of metallic nanowires with different orientation. Guti Lixue Xuebao/Acta Mech Solida Sin 32:433–439
40. Ma B, Rao Q-H, He Y-H (2014) Effect of crystal orientation on tensile mechanical properties of single-crystal tungsten nanowire. Trans Nonferrous Metals Soc China 24:2904–2910
41. Zhang J-M, Ma F, Xu K-W, Xin X-T (2003) Anisotropy analysis of the surface energy of diamond cubic crystals. Surf Interface Anal 35:805–809
42. Tsuzuki H, Rino JP, Branicio PS (2011) Dynamic behaviour of silicon carbide nanowires under high and extreme strain rates: a molecular dynamics study. J Phys D Appl Phys 44:055405
43. Chowdhury EH, Rahman MH, Jayan R, Islam MM (2021) Atomistic investigation on the mechanical properties and failure behavior of zinc-blende cadmium selenide (CdSe) nanowire. Comput Mater Sci 186:110001
44. Pial TH, Rakib T, Mojumder S, Motalab M, Akanda MAS (2018) Atomistic investigations on the mechanical properties and fracture mechanisms of indium phosphide nanowires. Phys Chem Chem Phys 20:8647–8657
45. Adachi S (2017) III-V ternary and quaternary compounds. In: Kasap S, Capper P (eds) Springer Handbook of Electronic and Photonic Materials. Springer International Publishing, Cham, pp 1–1